

AN XPS STUDY OF XeF_2 DRY ETCHING OF TUNGSTEN SILICIDE

E. GROSSMAN, A. BENSAOULA and A. IGNATIEV

Department of Physics, University of Houston, Houston, TX 77004, USA

Received 21 July 1987; accepted for publication 2 November 1987

X-ray photoelectron spectroscopy (XPS) and quartz crystal microbalance (QCM) measurements have been used to study the etching of $\text{WSi}_{0.6}$ by XeF_2 . Preferential etching of Si was observed for spontaneous etching and ion beam assisted etching. The Si removal from the WSi matrix created defects which enhanced the spontaneous etch rate by up to 30 times over that of the W(100) etch rate. The surface composition of $\text{WSi}_{0.6}$ changed under XeF_2 exposure with the observation of WF, SiF and SiF_3 as well as the volatile reaction product SiF_4 which was trapped in the reaction layer.

1. Introduction

The refractory metal silicides have been increasingly used lately in the VLSI technology as diffusion barriers, gate materials and electrical contacts. Studies of the silicides have been concentrated mainly on their electrical properties and the fabrication techniques like plasma etching or reactive ion etching (RIE) [1–5]. RIE of silicides using halides [6,7] has been studied with emphasis on the effect of parameters like gas pressure or halides concentration on the etch rate or the etching selectivity, while less attention was given to fundamental etching mechanisms.

Such mechanisms, with specific recent interest in halogen based etching, can be studied by the application of surface techniques like Auger electron spectroscopy (AES) and X-ray photoelectron spectroscopy (XPS). AES and XPS have been widely used for investigating the surface modification of silicides by ion beam sputtering [8–11], but there is no information on the surface modification of silicides after halogen-based chemical etching. The knowledge of the surface composition under halogen etching is also important from a practical point of view. Nonvolatile fluorinated compounds left on the surface may affect the performance of the device fabricated on the etched surface, or may cause corrosion in metal overlayers deposited subsequent to a fluorine etch [12]. In the present paper we report a detailed XPS study of $\text{WSi}_{0.6}$ etching by XeF_2 . The $\text{WSi}_{0.6}$ can be used as a gate material because of the stability of its Schottky barrier height and ideality factor during high

temperature source/drain implant anneal [1,13,14]. The tungsten silicide was investigated under spontaneous etching by XeF_2 , simultaneous etching under XeF_2 exposure and Ar ion beam exposure, and also for comparison, the silicide was physically sputtered by an Ar ion beam. The surface species and surface modifications, were studied by monitoring the Si 2p, W 4f and F 1s lines.

2. Experimental

The sputter deposited $\text{WSi}_{0.6}$ films were etched at room temperature in an ultra-high vacuum chamber under the following conditions: (i) spontaneous etching – exposure of the films to XeF_2 at a pressure of 4×10^{-6} Torr, (ii) ion beam assisted etch (IBAE) – exposure to XeF_2 (4×10^{-6} Torr) simultaneously with Ar^+ (4×10^{-5} Torr, 5 μA) ion beam bombardment, and (iii) physical sputtering – exposure of the $\text{WSi}_{0.6}$ films to Ar^+ ion beam of 2 kV at 4×10^{-5} Torr. All experiments were performed for periods of from 20 to 640 s.

Since XeF_2 is a highly reactive gas it was difficult to measure the exact pressure. However, relative measurements were accurate to 5% with total exposures of 80–2560 L (1 L = 10^{-6} Torr · s) measured by using an uncalibrated ion gauge.

The etched surfaces were examined in-situ by XPS right after the XeF_2 exposure. The XPS system employed an Mg $\text{K}\alpha$ X-ray source and a double pass cylindrical mirror analyzer (CMA) for electron energy analysis with a resolution of 1.2 eV. A value of 84.0 eV for the Au $4f_{7/2}$ line was used as a calibration for XPS binding energies (BE). The F 1s, Si 2p and W 4f spectra measured after the exposure, were also compared to those lines obtained from pure Si(111) and pure W(100) samples exposed to XeF_2 under the same conditions.

Prior to fluorine etching, the samples were sputter-cleaned and then annealed in 3×10^{-10} Torr to 800 °C for 30 min in order to restore their original composition of $\text{WSi}_{0.6}$ as measured by XPS.

The etch rates of the $\text{WSi}_{0.6}$ and W(100) were measured by depositing these materials onto quartz crystals which were then mounted on a microbalance holder (QCM) and monitoring the change in crystal frequency during the etch experiments.

3. Results and discussion

Fig. 1 shows F 1s spectra taken from spontaneous etched $\text{WSi}_{0.6}$ after different XeF_2 exposures. Exposure to XeF_2 for 80 L (curve a) resulted in a broad peak indicating a superposition of several fluorine chemical states.

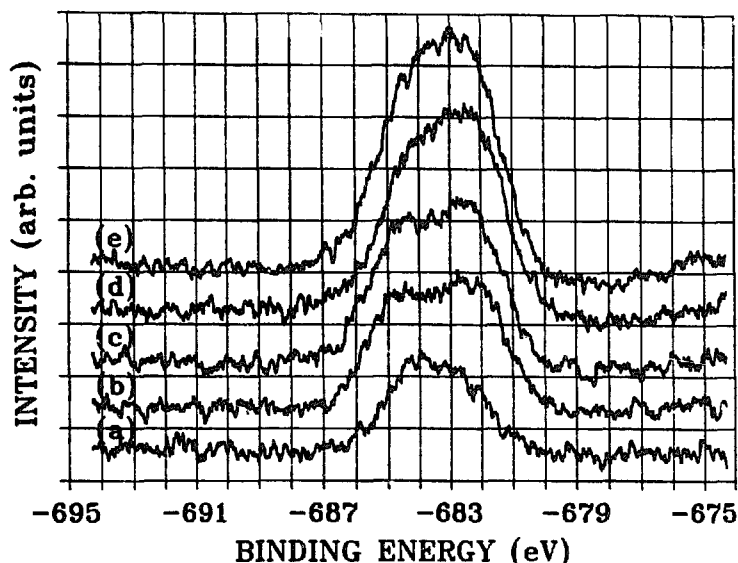


Fig. 1. F 1s photoelectron spectra after exposing $\text{WSi}_{0.6}$ to XeF_2 for (a) 80 L, (b) 240 L, (c) 480 L, (d) 960 L and (e) 1760 L.

Increasing the etching time (curves b–e) results in a change in the F 1s line shape with the high binding energy (BE) components decreasing relatively to the low BE components intensity. The low BE components were assigned to W–F bonds [16] and therefore the high BE components are attributed to Si–F bonds and a decrease in their concentration should reflect a decrease in the Si concentration on the $\text{WSi}_{0.6}$ film. This effect can be seen in fig. 2. Fig. 2 shows the W 4f and Si 2p normalized signal intensities plotted versus spontaneous etching time. The intensity was determined by first subtracting a linear background from the spectra and integrating by summation of all data points within the peak. The decrease in the silicon concentration reflects the preferential spontaneous etching of the $\text{WSi}_{0.6}$ exposed to XeF_2 . The etching rate of the silicon is high in the first 240 L and decreases with time until it reaches the W etching rate (after about 800 L). Comparison of the curves of fig. 1 to those of fig. 2 shows the correlation between the reduction of the F 1s high BE components to the reduction in the Si concentration.

The $\text{WSi}_{0.6}$ samples were exposed also to XeF_2 simultaneously with Ar^+ ion beam bombardment, i.e. ion beam assisted etching. Fig. 3 shows the F 1s spectra taken after IBAE for XeF_2 exposures of from 80 to 1760 L. As was seen for spontaneous etching (fig. 1) the F 1s spectrum is composed of contributions from WF_x and SiF_y compounds. However, in the case of IBAE the intensities of the higher BE components, which are attributed to SiF_y compounds, decrease faster with etch time than under spontaneous etch. This difference indicates higher preferential etching of the Si in the IBAE process, as will be shown later by the decrease of the Si/W concentration ratio with

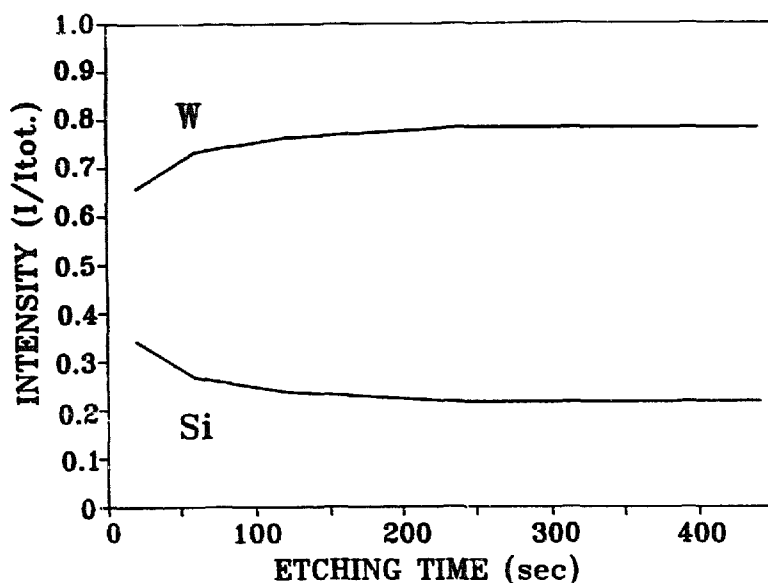


Fig. 2. W 4f and Si 2p normalized signal intensities from $\text{WSi}_{0.6}$ exposed to XeF_2 , versus etching time.

etch time. The IBAE also changes the composition of the silicon fluoride species remaining in the reaction layer from high to low fluorine concentration compounds (e.g. less of SiF_4 and more of SiF). This compositional change is due to not only a pure sputtering process but also to a chemical process. The ions which create surface defects create also a new supply of fluorine through

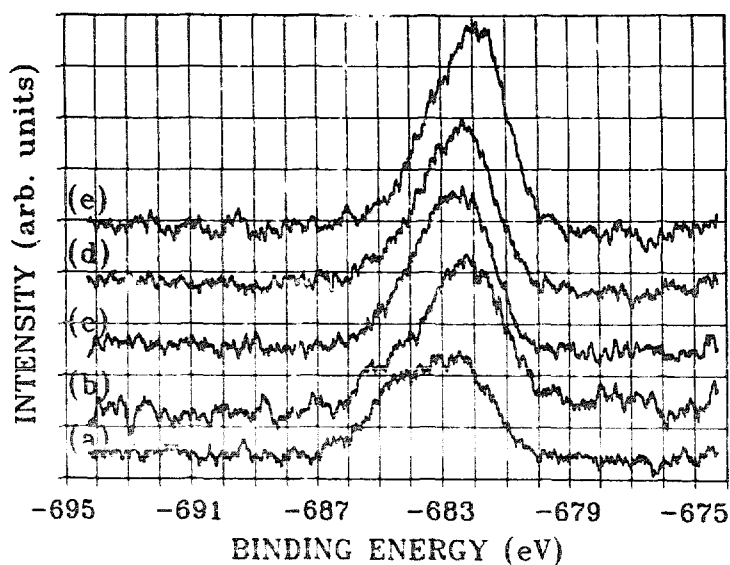


Fig. 3. F 1s photoelectron spectra after exposing $\text{WSi}_{0.6}$ to XeF_2 simultaneously with Ar^+ ion beam bombardment (IBAE): (a) 80 L, (b) 240 L, (c) 480 L, (d) 960 L and (e) 1760 L.

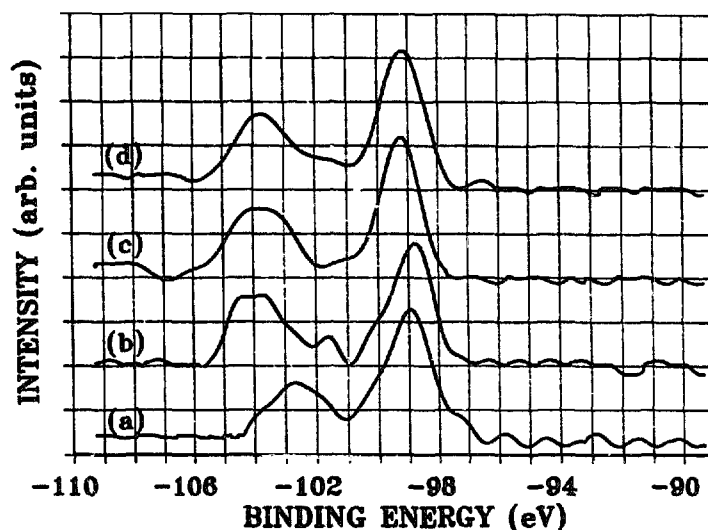


Fig. 4. Si 2p photoelectron spectra after exposing $\text{WSi}_{0.6}$ to XeF_2 for (a) 80 L, (b) 240 L, (c) 480 L and (d) 960 L.

the mobilization of fluorine from surface localized SiF , moving the reaction towards the formation of the volatile SiF_4 thus enhancing the etch rate of the Si.

The IBAE was performed without a differentially pumped ion gun. This could result in a formation of fluorine ions (by up to 10% of the total ions) and could affect the interpretation of the IBAE mechanism. However, we believe that the role of the ionized XeF_2 in the IBAE mechanism is insignificant. Previous experiments [18] of IBAE of W(100) using XeF_2 showed that decreasing the XeF_2 concentration from 10% to 1% (by increasing the Ar partial pressure by a factor of 10 and keeping the ion density constant) did not affect the etch rate. This emphasizes the role of the Ar ions in the IBAE process (e.g. creating defects on the surface, enhancing the XeF_2 molecules dissociation, enhancing the fluorinated species mobility, and more) and shows that even if fluorine ions are formed in the IBAE system their existence does not affect the interpretation of the IBAE mechanism.

The Si 2p spectra obtained from $\text{WSi}_{0.6}$ exposed to XeF_2 are shown in fig. 4. The spectra are composed of the main line at 99.2 eV and features at higher binding energies. After exposure of 80 L (curve a) the chemically shifted features are about 3.5 eV above the main unshifted line, and at higher exposures (curves b–d) they are shifted to higher BE by up to 4.7 eV. It has been demonstrated before [15] that mono-, di-, tri- and tetrafluorosilyl groups will include binding energy shifts in the Si 2p level of about 1 eV per fluorine atom. The intensity of each fluorinated silicon compound in the WSi etched surface can, as a result, be calculated by curve fitting of the Si 2p spectrum. The chemical shifts for the fluorinated Si compounds were chosen from the

Table 1

Peak position relative to the Si^0 line and full width at half maximum (FWHM) which were used for the curve fitting of the Si 2p lines

	ΔE (eV)	FWHM (eV)
Si	0	1.5
SiF	1.00	1.75
SiF ₂	2.05	2.0
SiF ₃	3.26	2.25
SiF ₄	4.70	2.5

work of McFeely et al. [15] for Si(111) exposed to XeF_2 . The peak position and full width at half maximum (FWHM) for each compound is summarized in table 1. By keeping those parameters constant and changing only the intensities of the individual peaks, a best fit was obtained. The results of the fit, shown in fig. 5, indicate that at an exposure of 80 L, the fluorinated silicon compounds in the surface layer were mainly SiF, SiF₃ and SiF₄ and small amount of SiF₂. At exposures above 240 L, the amounts of SiF and SiF₃ on the surface were reduced and the main fluorinated silicon compound became SiF₄. SiF₄ is the major reaction product in the fluorine etch of silicon and the increase of its content at the surface of WSi reflects the increase in the Si etch rate. The SiF₄ is a volatile molecule at room temperature and its existence indicates that SiF₄ is trapped in the surface reaction layer of the silicide, and that the silicon etch is proceeding through the formation of the silicon-tetrafluoride molecules and their diffusion through the reaction layer.

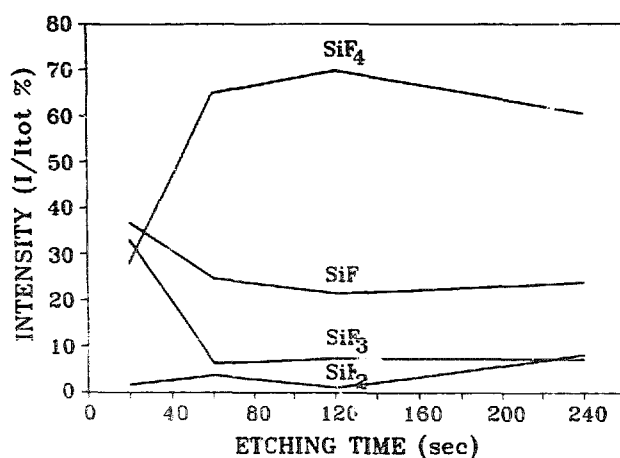


Fig. 5. SiF_x ($1 \leq x \leq 4$) compounds normalized intensity plotted versus etching time. The intensity was calculated from the results of the curve fitting of the Si 2p spectra obtained from the WSi etched surface.

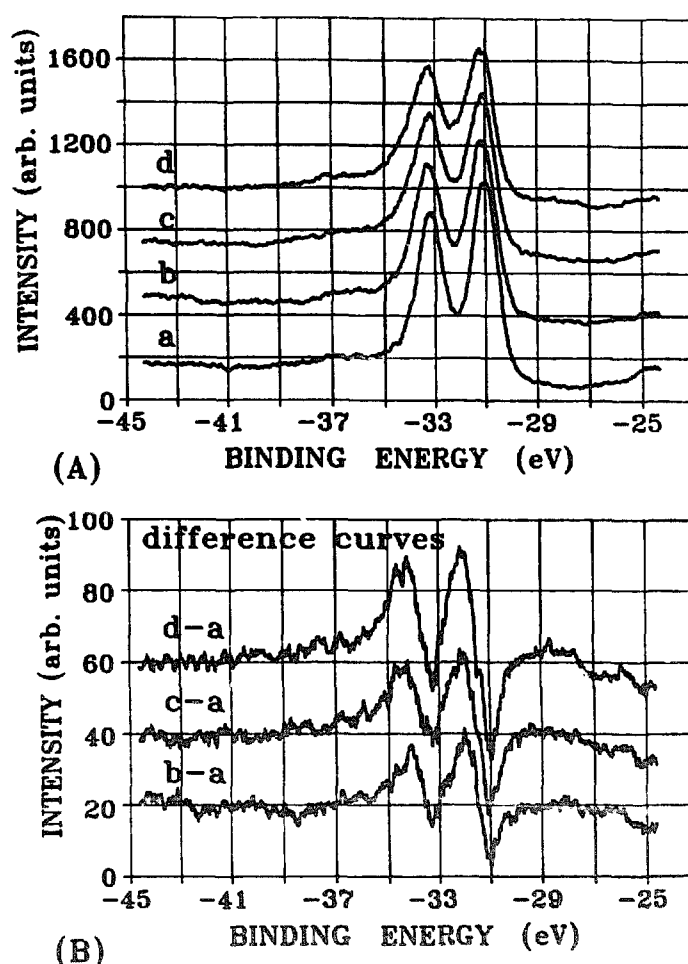


Fig. 6. (A) W 4f photoelectron spectra of: annealed $\text{WSi}_{0.6}$ (a), and $\text{WSi}_{0.6}$ exposed to XeF_2 for 80 L (b), 240 L (c) and 480 L (d). (B) Difference curves for spectra of (A).

The W 4f spectra from the WSi surface exposed to XeF_2 (fig. 6a) show minor shifts in the BE. The major difference observed is an addition of higher BE component which cause an asymmetry in the W 4f peak. This is more clearly shown in the W 4f difference curves of fig. 6b which is result of subtraction of a reference W 4f spectrum (obtained from annealed and unexposed WSi surface – fig. 6a, curve a) from the spectra obtained at different XeF_2 exposures. The difference curves show that the main extra feature is located at about 32 eV. Previous studies [16] have shown that the fluorination of tungsten to obtain tungsten hexafluoride induces a shift of 6.5 eV in the W 4f line and that a shift of near 1 eV is due to the formation of WF. As a result the high BE feature in the W 4f line can be identified as WF.

The sputtering of silicides is known to induce surface metal enrichment [8,10] by a preferential sputtering of the silicon. In the present study we have

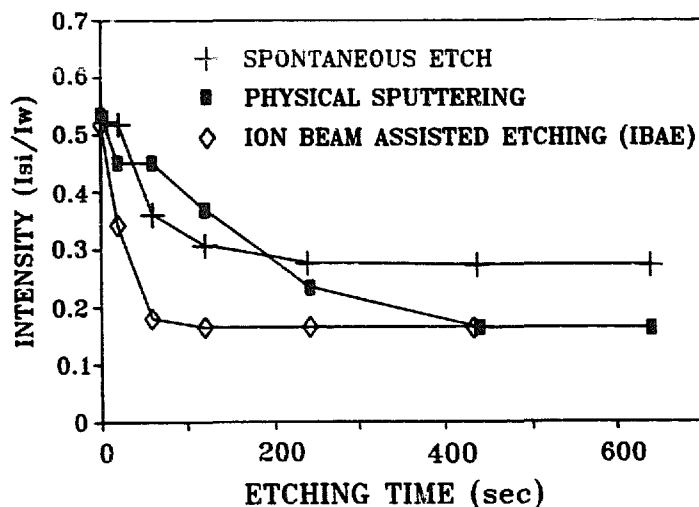


Fig. 7. Si/W ratio calculated from the Si 2p and W 4f lines plotted versus etching time, for physical sputtering, spontaneous etching and ion beam assisting etching (IBAE).

found similar effects due to sputtering, due to spontaneous etch and due to IBAE of the $\text{WSi}_{0.6}$. Fig. 7 shows the effect of the different etching methods on the W surface enrichment phenomenon. Spontaneous etch of WSi results in a small decrease in the Si/W ratio after 20 s of etching and a dramatic decrease after 60 s. Continuation of the etching process causes a further depletion of the Si with a final leveling of the surface composition at a Si to W ratio of 0.27. IBAE causes a more drastic change in the Si preferential etch and in the equilibrium surface concentrations. In the IBAE case there is no

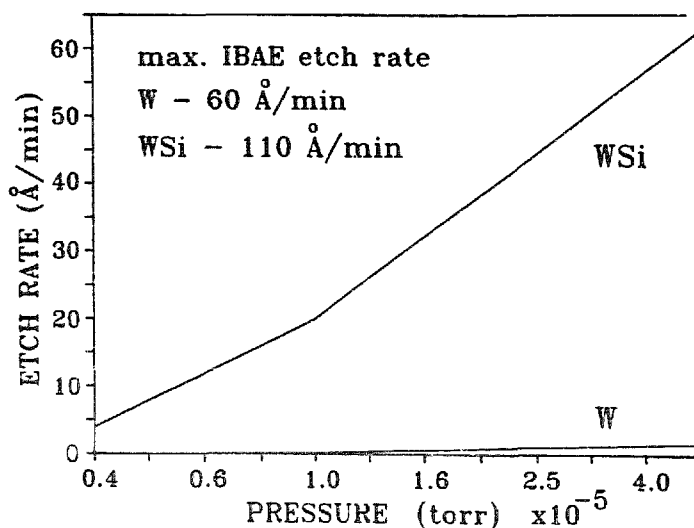


Fig. 8. Spontaneous etch rate of $\text{WSi}_{0.6}$ and W(100) versus XeF_2 pressure. Also indicated is the maximum etch rate achieved using IBAE technique.

Table 2

Spontaneous etch, IBAE and sputtering rates of $\text{WSi}_{0.6}$, W(100) and Si exposed to XeF_2

	Rate ($\text{\AA}/\text{min}$)		
	Spontaneous	IBAE	Sputtering
$\text{WSi}_{0.6}$	62	110	21
W(100)	2	60	7
Si ^{a)}	5	55	2

^{a)} Ref. [19].

Note the different exposure conditions for the Si: XeF_2 flow = 2×10^{-15} molecules/s, Ar^+ energy and current of 450 eV and 2.5 μA .

delay time for the Si depletion zone formation and the Si/W ratio decreases to a lower equilibrium level of $\text{Si}/\text{W} = 0.165$ after only 60 s of etching. Comparison of physical sputtering to both etching techniques shows a slower preferential sputtering rate for Si but the equilibrium concentration levels are as low as those for IBAE.

Fig. 8 shows the spontaneous etch rates of $\text{WSi}_{0.6}$ and of W(100) [16] plotted versus XeF_2 pressure. In both materials the etch rates increased with increasing pressure, however, the $\text{WSi}_{0.6}$ etch rate was up to 30 times greater than the W(100) etch rate (see also table 2). The preferential removal of the Si atoms from the WSi matrix creates defects in the silicide. As was shown for W etching [17], the creation of defects in the surface region enhances the formation of the volatile fluorinated compounds which leads to higher etching rates. IBAE causes increases in the etch rates of both WSi and W(100). It should be noted however, that while the tungsten IBAE rate showed a dramatic enhancement effect of up to 30 times over the spontaneous etch rate, the WSi IBAE rate was increased by only about 2 times over the spontaneous rate. This difference in the enhancement of the etch rate indicates that the WSi has already been damaged by the Si removal and additional damage did not affect the etch rate as drastically as for W(100).

4. Conclusions

XPS and QCM were used to study the fluoride etching of $\text{WSi}_{0.6}$. It has been shown that the preferential removal of Si from the tungsten silicide matrix, a process well documented in physical sputtering, occurs also in chemical etching. This preferential etching creates silicon related defects in the $\text{WSi}_{0.6}$ matrix which cause enhancement of the $\text{WSi}_{0.6}$ spontaneous etch rate by up to 30 times over that of W(100). For low exposure of XeF_2 (80 L) the surface composition was characterized by WF, and SiF , SiF_3 and SiF_4 . Larger exposures (above 240 L) increased the amount of SiF_4 which was trapped in the reaction layer.

References

- [1] Z. Zhongde, N.W. Cheung, Z.J. Lemnois, M.D. Starthman and J.B. Stimmel, *J. Vacuum Sci. Technol.* B4 (1986) 1398.
- [2] S.P. Murarka, *J. Vacuum Sci. Technol.* B4 (1986) 1325.
- [3] G.A. Mattiussi, *J. Vacuum Sci. Technol.* B4 (1986) 1352.
- [4] D.G. Hemmes, *J. Vacuum Sci. Technol.* B4 (1986) 1332.
- [5] T.P. Chow and A.J. Steckl, *J. Electrochem. Soc.* 131 (1984) 2325.
- [6] M. Zhang, J.Z. Li, I. Adesida and E.D. Wolf, *J. Vacuum Sci. Technol.* B1 (1983) 1037.
- [7] K.C. Cadogan, S. Sivaram and C.D. Reintsema, *J. Vacuum Sci. Technol.* A4 (1986) 739.
- [8] S. Valeri, U. del Pennino and P. Lomellini, *Thin Solid Films* 130 (1985) 315.
- [9] R. Pantel and F.A. d'Avitaya, *Thin Solid Films* 140 (1986) 177.
- [10] Th. Wirth, V. Atzrodt and H. Lange, *Phys. Status Solidi* 82 (1984) 459.
- [11] V. Atzrodt, W. Titel, Th. Wirth and H. Lange, *Phys. Status Solidi* 75 (1983) K15.
- [12] P.K. Charvat, E.E. Krueger and A.L. Ruoff, *J. Vacuum Sci. Technol.* B4 (1986) 812.
- [13] T. Ohnishi, N. Yokoyama, H. Onodera, S. Suzuki and A. Shibatomi, *Appl. Phys. Letters* 43 (1983) 601.
- [14] T.N. Jackson and J.F. DeGelormo, *J. Vacuum Sci. Technol.* B3 (1985) 1676.
- [15] F.R. McFeely, J.F. Morar and F.J. Himpsel, *Surface Sci.* 165 (1986) 277.
- [16] A. Bensaoula, E. Grossman and A. Ignatiev, *J. Appl. Phys.* 62 (1987) 4587.
- [17] A. Bensaoula, J.A. Strozier, A. Ignatiev, J. Yu and J.C. Wolfe, *J. Vacuum Sci. Technol.* A5 (1987) 1921.
- [18] Unpublished data.
- [19] J.W. Coburn and H.F. Winters, *J. Appl. Phys.* 50 (1979) 3189.